HHS Public Access

Author manuscript

Nat Methods. Author manuscript; available in PMC 2014 September 03.

Published in final edited form as:

Nat Methods. 2014 March ; 11(3): 313–318. doi:10.1038/nmeth.2835.

Multiplexed 3D Cellular Super-Resolution Imaging with DNA-PAINT and Exchange-PAINT

R. Jungmann[1,2,*], **M.S. Avendano**[1,2,*], **J.B. Woehrstein**[1,*], **M. Dai**[1,5], **W.M. Shih**[1,3,4], and **P. Yin**[1,2]

[1]Wyss Institute for Biologically Inspired Engineering, Harvard University, Boston, Massachusetts 02115, USA

[2]Department of Systems Biology, Harvard Medical School, Boston, Massachusetts 02115, USA

[3]Department of Biological Chemistry and Molecular Pharmacology, Harvard Medical School, Boston, Massachusetts 02115, USA

[4]Department of Cancer Biology, Dana-Farber Cancer Institute, Boston, Massachusetts 02115, USA

[5]Program in Biophysics, Harvard University, Cambridge, Massachusetts 02138, USA

Abstract

While super-resolution fluorescence microscopy is a powerful tool for biological research, obtaining multiplexed images for a large number of distinct target species remains challenging. Here we use the transient binding of short fluorescently labeled oligonucleotides (DNA-PAINT, point accumulation for imaging in nanoscale topography) for simple and easy-to-implement multiplexed 3D super-resolution imaging inside fixed cells and achieve sub-10 nm spatial resolution *in vitro* using synthetic DNA structures. We also report a novel approach for multiplexing (Exchange-PAINT) that allows sequential imaging of multiple targets using only a single dye and a single laser source. We experimentally demonstrate ten-"color" super-resolution imaging *in vitro* on synthetic DNA structures and four-"color" imaging of proteins in a fixed cell.

Far-field fluorescence microscopy has seen major advances since the advent of methods circumventing the classical diffraction limit, i.e. super-resolution microscopy[1,2]. Most implementations "switch" molecules between fluorescent ON- and OFF-states to obtain sub-diffraction image resolution. This switching is traditionally obtained in two ways: "targeted"

Correspondence should be addressed to P.Y. (py@hms.harvard.edu).

*Authors contributed equally.

Note: Supplementary information is available in the online version of the paper.

Author Contributions: R.J., M.S.A., and J.B.W. contributed equally to this work. R.J. and M.S.A conceived the study, designed and performed the experiments, analyzed the data, and wrote the manuscript. J.B.W. designed and performed the experiments, analyzed the data, and wrote the manuscript. M.D. performed the experiments, analyzed the data, and developed the drift correction software. W.M.S. supervised the project, discussed the results and critiqued the paper. P.Y. conceived, designed, and supervised the study, interpreted the data and wrote the manuscript. All authors reviewed and approved the manuscript.

Competing Financial Interests: The authors declare competing financial interests: a provisional US patent application has been filed.

switching actively confines the fluorescence excitation to an area smaller than the diffraction of light (e.g. stimulated emission depletion microscopy or STED[3]), whereas "stochastic" switching uses photoswitchable proteins (photoactivated localization microscopy or PALM[4]) or photoswitchable organic dyes (e.g. stochastic optical reconstruction microscopy or STORM[1]). Although these methods offer unprecedented spatial resolution, they tend to be technically involved to implement, and multiplexing for a large number of distinct targets is generally challenging.

Point accumulation for imaging in nanoscale topography (PAINT)[5-7] provides an alternative stochastic super-resolution imaging method. Here, imaging is carried out using diffusing fluorescent molecules that interact transiently with the sample. This method is straightforward to implement and does not require specialized equipment or conditions to obtain photoswitching, thus making it more accessible to laboratories with standard instrumentation and sample preparation capabilities compared to STED or STORM. Initially, PAINT was applied to obtain super-resolved images of cell membranes[5] and artificial lipid vesicles[5]. However a key limitation of PAINT's original formulation is that dyes interact with the sample via electrostatic coupling or hydrophobic interactions. This limits the availability of PAINT-compatible dyes, making it hard to simultaneously image specific biomolecules of interest. Recently, PAINT has been implemented based on continuously and stochastically labeling specific membrane biomolecules with fluorescent ligands (e.g. antibodies)[6]. The approach, termed universal PAINT (uPAINT), achieves specific dye-sample interactions but still lacks the ability to specify interactions with programmable kinetics. Similar to PAINT, binding of DNA intercalating dyes has also been used to obtain super-resolved images of DNA[8,9].

To achieve programmable dye interactions and to increase the specificity and the number of utilizable fluorophores, DNA-PAINT was developed[10]. Here, stochastic switching between fluorescence ON- and OFF-states is implemented via repetitive, transient binding of fluorescently labeled oligonucleotides ("imager" strands) to complementary "docking" strands (Fig. 1a, b). In the unbound state, only background fluorescence from partially quenched[10] imager strands is observed (Fig. 1a). However, upon binding and immobilization of an imager strand, fluorescence emission is detected using total internal reflection (TIR) or highly inclined and laminated optical sheet (HILO) microscopy[11]. DNA-PAINT enhances PAINT's simplicity and ease-of-use with the programmability and specificity of DNA hybridization. Importantly, it enables widely adjustable fluorescence ON- and OFF-times by tuning the binding strength and concentration of the imager strand[10]. DNA-PAINT has been used to obtain multicolor sub-diffraction images of DNA nanostructures[10,12-15] with ≈25 nm spatial resolution[14]. Spectral multiplexing is straightforward as no external photoswitching of dyes is necessary, and imaging specificity is obtained through orthogonality of DNA sequences coupled to spectrally distinct dyes[13].

Here, by linking DNA-PAINT docking strands to antibodies, we extend the DNA-PAINT method to enable multiplexed two- and three-dimensional super-resolution imaging of protein components in fixed cells. We also report sub-10 nm lateral imaging resolution *in vitro* of synthetic DNA structures, without the use of a sophisticated setup (e.g. as in STED[3] or dual-objective STORM[16]) or specialized experimental conditions such as dye-caging

approaches[17]. Finally, we use the unique programmability of DNA molecules to perform sequential multiplexing (Exchange-PAINT) using only a single fluorescent dye and obtain the first ten-"color" *in vitro* super-resolution image using DNA nanostructures. We also show the applicability of Exchange-PAINT to cellular imaging by demonstrating four-"color" imaging of protein targets in fixed cells and three-"color" 3D imaging.

Results

Sub 10-nm *in vitro* imaging with DNA-PAINT

First, we optimized the spatial resolution of DNA-PAINT and imaged DNA origami structures that mimic *in vitro* assembled microtubules (Fig. 1a). In DNA origami, a long single-stranded DNA molecule (i.e. the "scaffold") is "folded" into a desired shape or pattern by the sequence-specific binding of hundreds of short oligonucleotides (i.e. the "staple" strands) to designated regions on the scaffold[18,19] (Supplementary Figure 1). The DNA origami monomer is a tunnel-like structure (dimensions ≈16 nm by ≈16 nm by ≈75 nm). Monomers were linked using connector strands to form a homo-polymer mimicking microtubules (Fig. 1c), which formed with high yield (Supplementary Figure 2). To allow for DNA-PAINT imaging, staple strands on two opposite faces of the structure were extended with single-stranded docking sites at the 3′-end. Assembled polymers were bound to a BSA-biotin-streptavidin glass surface using biotinylated staple strands extruding from the bottom of the structure[10,13,14,20]. DNA-PAINT was then performed using Cy3b-labeled imager strands.

The super-resolved image reveals two adjacent lines spaced ≈16 nm apart, matching the designed microtubule-like geometry (Fig. 1d). The cross-sectional profiles of two regions of interests possess well-separated peaks at the designed distance with a full width at half maximum (FWHM) of ≈7–10 nm (Fig. 1e, see also Supplementary Figure 3 for a large field of view image and a diffraction-limited representation). We note that this resolution was obtained in standard DNA hybridization buffer without the use of oxygen scavengers[21], triplet-state quenchers[22], or redox systems[23]. The increase in spatial resolution compared to earlier DNA-PAINT studies[10,13-15] is obtained by enhanced drift correction and higher localization accuracy. The latter is achieved by collecting more emitted photons per binding event through optimizing fluorescence ON-times and camera integration time, and increasing laser excitation intensities. Extracting more photons per binding event is also facilitated by the fact that DNA-PAINT imaging is not prone to photobleaching, as imager strands are continuously replenished from solution[10]. This replenishing also allows near 100 % imaging efficiency of all docking sites[10]. This imaging efficiency of docking sites does not necessarily translate to imaging efficiency of targets, as labeling efficiency of targets with docking strands may not be 100 %. However, if present and accessible, every docking site should eventually be imaged during data acquisition[10].

Straightforward extension to multicolor imaging was obtained by coupling spectrally distinct dyes to orthogonal imager strand sequences as reported previously[13] (see Supplementary Figure 4 for three-color image of microtubule-like DNA origami polymers). The orthogonality of the imager strand sequences prevents crosstalk between different color channels (Supplementary Figure 4b–d).

Multiplexed cellular super-resolution imaging with DNA-PAINT

To image cellular components with DNA-PAINT, protein targets were specifically labeled using antibodies conjugated with DNA docking strands (Fig. 2). Conjugates are formed by first reacting biotinylated docking strands with streptavidin, and then incubating with biotinylated antibodies. We first immunostained fixed HeLa cells using a preassembled antibody-DNA conjugate against beta-tubulin. ATTO655-labeled imager strands were then introduced, and imaging was performed using HILO[11]. The resulting super-resolution images show a clear increase in spatial resolution over the diffraction-limited representation (Fig. 2a–c). A cross-sectional profile at position <i> in Fig. 2b yields a distance of ≈79 nm between two adjacent microtubules with an apparent width of ≈47 and ≈44 nm for each (see Supplementary Figure 5 for quantification and higher magnification image), consistent with earlier reports[24]. We observed little-to-no non-specific binding of imager strands to non-labeled cellular components (see later paragraphs for quantitative characterization and discussion of non-specific binding).

Multicolor imaging is achieved by using orthogonal imager strands coupled to spectrally distinct dyes. We labeled microtubules in a fixed HeLa cell with a preassembled antibody-DNA conjugate carrying a docking sequence for Cy3b-labeled imager strands, and stained mitochondria using a second antibody linked to an orthogonal sequence for ATTO655-labeled imager strands (Fig. 2d). While both Cy3b- and ATTO655-labeled imager strands co-existed in solution, imaging was performed sequentially. Images were drift-corrected and different color channels were aligned using gold nanoparticles as fiducial markers (see Online Methods for details). The resulting super-resolution images showed a clear increase in spatial resolution as compared to the diffraction-limited representation and no crosstalk between colors was observed (Fig. 2d–f).

Ten-“color” super-resolution imaging with Exchange-PAINT

As imager strands only transiently bind to the docking strands, DNA-PAINT allows for a new multiplexing approach where orthogonal imager strands are sequentially applied to the same sample. This approach, which we call Exchange-PAINT, is depicted in Fig. 3a. Initially, different target species are labeled with orthogonal docking strands. Once all components are labeled, the first imager strand species P1* (complementary to docking strands P1) is introduced and a DNA-PAINT image is acquired only for the targets labeled with P1. In a subsequent washing step, imager strands P1* are removed and imager strands P2* are introduced. Another image for only P2 is then acquired. In each imaging step, the respective docking sites are super-resolved and a unique pseudocolor is assigned. Washing and imaging steps are repeated until all desired targets are imaged. These images are then aligned and combined to produce the final “multi-color” image for the entire sample.

Unlike the spectral multiplexing approach described in the previous section, in Exchange-PAINT, the same dye and hence the same laser is used for all the target species. As such, multiplexing is limited only by the number of possible orthogonal DNA docking sequences instead of the number of spectrally distinct dyes (a typical limit for most previous fluorescence imaging methods).

Using Exchange-PAINT, we obtained ten-"color" super-resolution images for DNA structures. We designed ten unique rectangular DNA origamis[18], each displaying a distinct pattern of orthogonal docking strands that resembles a digit between 0 and 9 (see Fig. 3b for pattern 4). After surface immobilization of all ten structures, sequential imaging was performed using a custom-made fluidic chamber (Supplementary Figure 6a) for easy liquid handling. Ten orthogonal imager strands (P1* to P10*), all labeled with Cy3b, were used to perform Exchange-PAINT. The resulting digits from all ten imaging rounds are shown in Fig. 3c. Each target is resolved with high spatial resolution. Cross-sectional histograms along the bars of the digits show sub-10 nm FWHM of the distributions (data not shown), similar to Fig. 1d and e. Note that high resolution is maintained for all digits, as the same optimized dye (Cy3b) and imaging conditions are used in each cycle.

Fig. 3d shows a combined image of all ten rounds, demonstrating specific interaction of imager strands with respective targets with no observable crosstalk between cycles. Digits 8 and 9 are not present in the selected area (see Supplementary Figure 7 for the full image which includes all 10 digits). An apparent "green" digit 5 instead of 2 was observed (<i> in Fig. 3d). This is likely not a falsely imaged digit 5 from crosstalk, but rather a "mirrored" digit 2 (see Supplementary Figure 8 for details and additional examples of mirrored digits). A mirrored image likely results from an origami immobilized upside-down[25], with docking strands trapped underneath, yet still accessible to imager strands.

The fluidic setup is designed to minimize sample movement by "decoupling" the fluid reservoir and syringe from the actual flow chamber via flexible tubing. To avoid sample distortion, special care was taken to ensure gentle fluid flow during washing steps. To verify that the sample indeed exhibited little movement and little-to-no distortion, we performed a ten-round Exchange-PAINT experiment. We imaged the DNA origami for digit 4 in the first round and reimaged it after ten rounds of buffer exchange. The total sample movement (physical movement of the fluidic chamber with respect to the objective) was less than 2 μm, which could easily be corrected using fiducial markers. Normalized cross-correlation analysis for select structures produced a correlation coefficient 0.92 (Supplementary Figure 9), demonstrating almost no sample distortion (also see the discussion in the cellular imaging section).

Finally, using Exchange-PAINT, we successfully imaged four different digit patterns on the same DNA origami structure (Fig. 3e, see also Supplementary Figure 10 for a large field of view image). Thus Exchange-PAINT is not limited to spatially separate species and can resolve sub-diffraction patterns on the same structure with no observable crosstalk or sample distortion. Aligning images from different Exchange-PAINT rounds is straightforward using DNA origami-based drift markers. Additionally, because imaging is performed using the same dye, no chromatic aberration needs to be corrected between imaging rounds.

Multiplexed 3D cellular imaging with Exchange-PAINT

We next demonstrated multiplexed *in situ* imaging in a fixed HeLa cell with Exchange-PAINT. Fig. 4a–e show four-"color" super-resolution images obtained by sequential imaging using only a single dye (ATTO655). Using custom-made fluidic chambers (Supplementary Figure 6b), we obtained super-resolution images of β-tubulin in

microtubules, COX IV in mitochondria, TGN46 in the Golgi complex, and PMP70 in peroxisomes. Also see Supplementary Figure 11 for additional images of microtubules and mitochondria. Imaging and washing was performed in a similar fashion as for DNA structures. Again, we see little-to-no non-specific binding of the imager strands to non-labeled components.

To quantify possible non-specific interactions of the imager strands with cellular components, we performed Exchange-PAINT experiments, where no DNA-PAINT docking strands were present on the antibody-streptavidin conjugates, but the "labeling" and imaging process was otherwise performed as described above (see Supplementary Figure 12). We observed minimal non-specific interaction of the imager strands (ATTO655 or Cy3b) with the cellular components including genomic DNA. Non-specific interactions can be excluded by analyzing their "blinking" behavior in the intensity vs. time trace[13]: they lead to non-repeating localization events, and hence show an easily identifiable blinking signature (non-exponential distribution of ON- and OFF-times) that differs from specific DNA hybridization interactions (see Supplementary Figure 12 for images and representative blinking signature of specific vs. non-specific interactions).

To quantify potential sample distortion in cellular Exchange-PAINT imaging, we performed a similar study as in the *in vitro* case. Here, we imaged microtubules and mitochondria in four rounds of Exchange-PAINT, by first imaging microtubules, then mitochondria and repeating the process. We then selected a region of interest in each image and performed a normalized cross-correlation analysis. We obtained a cross-correlation coefficient of 0.80 and 0.96 for the microtubule and mitochondria images, respectively (for details see Supplementary Figure 13), demonstrating minimal sample distortion.

We note, that even in a super-resolution image without liquid exchange, one cannot expect 100 % correlation between two consecutive images of the same region in a sample due to the stochastic nature of the image formation. To see this effect, one can simply split a super-resolution raw data set into two parts of equal length, perform a stochastic reconstruction, and calculate the normalized cross-correlation coefficient for these two supposedly equal images. We performed this analysis for a sub-region of the microtubule image in Fig. 4f and obtained a coefficient of 0.88, similar to the Exchange-PAINT case of 0.80 (Supplementary Figure 13).

Finally, we used optical astigmatism imaging[26,27] to demonstrate 3D Exchange-PAINT super-resolution imaging in a fixed HeLa cell. We labeled microtubules, mitochondria, and peroxisomes, and obtained three-"color" 3D super-resolution Exchange-PAINT images using Cy3b (Fig. 4f–h). Fig. 4i shows a zoomed-in image of the highlighted area in Fig. 4f, revealing separate microtubules crossing each other in different z planes (Fig. 4j). A cross-sectional histogram in z yields a distance of ≈109 nm, well below the diffraction limit (Fig. 4k). See also Supplementary Figure 14 for an additional 3D DNA-PAINT image of microtubules.

Discussion

We enhanced the capabilities of DNA-PAINT, achieving sub-10 nm resolution on par with other more sophisticated stochastic reconstruction methods[16] while avoiding the need for specialized optical setups or sample preparation methods[17]. We further demonstrated spectrally multiplexed DNA-PAINT in fixed cells in both two and three dimensions with high labeling specificity.

To obtain highly multiplexed super-resolution images, we introduced a simple and scalable approach called Exchange-PAINT, which uses only a single fluorescent dye and a single laser source. We demonstrated the first ten-"color" super-resolution image of synthetic DNA structures, and achieved a four-"color" *in situ* image of proteins in fixed cells. Here, the number of orthogonal DNA sequences, as opposed to the number of spectrally distinguishable dyes, limits the multiplexing capability. For a 9 nt imager strand, there could be several hundred non-interacting sequences within tight bounds for dissociation kinetics. Exchange-PAINT could thus potentially enable a significant increase in multiplexing for super-resolution as well as diffraction-limited imaging.

Sequential multiplexing as in Exchange-PAINT provides a complementary approach to previous spectral and geometric multiplexing[13,28]. Compared to geometric multiplexing[13,28], Exchange-PAINT uses a more compact labeling entity (a ∼9 nt DNA strand). Compared to spectral multiplexing[28,29], Exchange-PAINT uses only a single fluorophore, thus allowing the selection of an optimal dye with respect to its photophysical properties (e.g. number of emittable photons) for super-resolution imaging. Unlike previous multiplexing approaches for diffraction-limited imaging based on DNA strand exchange reactions[30] and in situ sequencing[31], Exchange-PAINT does not involve "labeling" and "erasing" steps, as imager strands only bind to docking strands transiently. Exchange-PAINT thus permits simpler experimental procedures and faster image acquisition (∼1–2 min of washing between imaging cycles) while preserving DNA-PAINT's intrinsic super-resolution capability.

To fully translate DNA-PAINT and Exchange-PAINT's *in vitro* imaging capability to *in situ* imaging of cellular components, it is important to further develop strategies to label diverse cellular targets with high specificity and efficiency. One way to facilitate this goal, as noted by other researchers[17,24,32], is reducing the label size. Our current antibody-DNA conjugation method based on streptavidin bridging, though providing a simple and modular approach, results in a rather bulky conjugate. Thus a next logical step would be direct coupling of primary antibodies to DNA strands[33] without a streptavidin intermediate. Additionally, to further decrease the label size, it would be advantageous to use nanobody- or aptamer-based labeling strategies[24,32], with the latter serving as a natural extension to DNA-PAINT imaging as it already uses nucleic acid-based interactions. In addition to protein imaging, our method should also be directly applicable to DNA and RNA imaging in fixed cells, e.g. by using fluorescence *in situ* hybridization methods[28,34].

DNA-PAINT and Exchange-PAINT provides a simple and robust method for highly multiplexed super-resolution imaging. With further development, we anticipate it will eventually become a useful and standard tool for studying complex biomolecular systems.

Online Methods

Materials

Unmodified DNA oligonucleotides were purchased from Integrated DNA Technologies. Fluorescently modified DNA oligonucleotides were purchased from Biosynthesis. Biotinylated monoclonal antibodies against β-tubulin and COX IV were purchased from Cell Signaling. Anti-PMP70 was purchased from Abcam. Anti-TGN46 was purchased from VWR. Streptavidin was purchased from Invitrogen (Catalog number: S-888). Bovine serum albumin (BSA), and BSA-biotin was obtained from Sigma Aldrich (Catalog Number: A8549). Glass slides and coverslips were purchased from VWR. Lab-Tek II chambered cover glass were purchased from Thermo Fisher Scientific. M13mp18 scaffold was obtained from New England Biolabs. p8064 scaffold for microtubule-like DNA origami structures was prepared as described before[19]. 'Freeze N Squeeze' columns were ordered from Bio-Rad. TetraSpeck Beads were purchased from Life Technologies. Paraformaldehyde, glutaraldehyde and TEM grids (FORMVAR 400 Mesh Copper Grids) were obtained from Electron Microscopy Sciences.

Three buffers were used for sample preparation and imaging: Buffer A (10 mM Tris-HCl, 100 mM NaCl, 0.05 % Tween-20, pH 7.5), buffer B (5 mM Tris-HCl, 10 mM $MgCl_2$, 1 mM EDTA, 0.05 % Tween-20, pH 8), and buffer C (1×PBS, 500 mM NaCl, pH 8).

Optical setup

Fluorescence imaging was carried out on an inverted Nikon Eclipse Ti microscope (Nikon Instruments) with the Perfect Focus System, applying an objective-type TIRF configuration using a Nikon TIRF illuminator with an oil-immersion objective (CFI Apo TIRF 100×, NA 1.49, Oil). For 2D imaging an additional 1.5 magnification was used to obtain a final magnification of ≈150-fold, corresponding to a pixel size of 107 nm. Three lasers were used for excitation: 488 nm (200 mW nominal, Coherent Sapphire), 561 nm (200 mW nominal, Coherent Sapphire) and 647 nm (300 mW nominal, MBP Communications). The laser beam was passed through cleanup filters (ZT488/10, ZET561/10, and ZET640/20, Chroma Technology) and coupled into the microscope objective using a multi-band beam splitter (ZT488rdc/ZT561rdc/ZT640rdc, Chroma Technology). Fluorescence light was spectrally filtered with emission filters (ET525/50m, ET600/50m, and ET700/75m, Chroma Technology) and imaged on an EMCCD camera (iXon X3 DU-897, Andor Technologies).

DNA origami self-assembly

The microtubule-like DNA origami structures were formed in a one-pot reaction with 40 μl total volume containing 10 nM scaffold strand (p8064), 500 nM folding staples and biotin handles, 750 nM biotin anti-handles and 1.1 μM DNA-PAINT docking strands in folding buffer (1×TAE Buffer with 20 mM $MgCl_2$). The solution was annealed using a thermal ramp[13] cooling from 80 °C to 14 °C over the course of 15 h. After self-assembly,

monomeric structures were purified by agarose gel electrophoresis (1.5 % agarose, 0.5×TBE, 10 mM $MgCl_2$, 1×SybrSafe) at 4.5 V/cm for 1.5 h (see Supplementary Figure 2). Gel bands were cut, crushed and filled into a 'Freeze 'N Squeeze' column and spun for 5 min at 1000×g at 4 °C. Polymerization was carried out at 30 °C for 48 h with a 5-fold excess of polymerization staples in folding buffer. Polymerized structures were used for imaging without further purification.

DNA origami drift markers were self-assembled in a one-pot reaction (40 μl total volume, 20 nM M13mp18 scaffold, 100 nM biotinylated staples, 530 nM staples with DNA-PAINT docking sites, 1×TAE with 12.5 mM $MgCl_2$). Self-assembled structures were purified as described before.

DNA origami structures for the 4-"color" *in vitro* Exchange-PAINT demonstration were self-assembled in a one-pot reaction (40 μl total volume, 30 nM M13mp18 scaffold, 470 nM biotinylated staples, 400 nM staples with docking sites for number imaging, 370 nM core structure staples, 1×TAE with 12.5 mM $MgCl_2$). Self-assembled structures were purified as described before.

DNA origami structures for the 10-"color" *in vitro* Exchange-PAINT demonstration were self-assembled in a one-pot reaction (40 μl total volume, 30 nM M13mp18 scaffold, 36 nM biotinylated staples, 750 nM staples with docking sites for number imaging, 300 nM core structure staples, 1×TAE with 12.5 mM $MgCl_2$). Structures were not purified. Excessive staples are washed out of the sample after immobilization of the structure on the surface.

Antibody-DNA conjugates

Antibody-DNA conjugates used to specifically label proteins of interest with DNA-PAINT docking sites were preassembled in two steps: First, 3.2 μl of 1 mg/ml streptavidin (dissolved in buffer A) was reacted with 0.5 μl biotinylated DNA-PAINT docking strands at 100 μM and an additional 5.3 μl of buffer A for 30 min at room temperature (RT) while gently shaking. The solution was then incubated in a second step with 1 μl of monoclonal biotinylated antibodies at 1 mg/ml against the protein of interest for 30 min at RT. Filter columns (Amicon 100 kDa, Millipore) were used to purify the preassembled conjugates from unreacted streptavidin-oligo conjugates.

Cell immunostaining

HeLa and DLD1 cells were cultured with Eagle's minimum essential medium fortified with 10 % FBS with penicillin and streptomycin and were incubated at 37 °C with 5 % CO_2. Approximately 30 % confluence cells per well were seeded into Lab-Tek II chambered cover glass 24 h before fixation. Microtubules, mitochondria, Golgi complex, and peroxisomes were immunostained using the following procedure: washing in PBS; fixation in a mixture of 3 % paraformaldehyde and 0.1 % glutaraldehyde in PBS for 10 min; 3-times washing with PBS; reduction with ≈1 mg/ml $NaBH_4$ for 7 min; 3-times washing with PBS; permeabilization with 0.25 % (v/v) Triton X-100 in PBS for 10 min; 3-times washing with PBS; blocking with 3 % (w/v) bovine serum albumin for 30 min and staining over night with the preassembled antibody-DNA conjugates against β-tubulin, COX IV, PMP70, or

TGN46 (conjugates were diluted to 10 μg/ml in 5 % BSA); 3-times washing with PBS; post-fixation in a mixture of 3 % paraformaldehyde and 0.1 % glutaraldehyde in PBS for 10 min; and 3-times washing with PBS.

Super-resolution DNA-PAINT imaging of microtubule-like DNA origami structures

For sample preparation, a piece of coverslip (No. 1.5, 18×18 mm^2, ≈0.17 mm thick) and a glass slide (3×1 $inch^2$, 1 mm thick) were sandwiched together by two strips of double-sided tape to form a flow chamber with inner volume of ≈20 μl. First, 20 μl of biotin-labeled bovine albumin (1 mg/ml, dissolved in buffer A) was flown into the chamber and incubated for 2 min. The chamber was then washed using 40 μl of buffer A. 20 μl of streptavidin (0.5 mg/ml, dissolved in buffer A) was then flown through the chamber and allowed to bind for 2 min. After washing with 40 μl of buffer A and subsequently with 40 μl of buffer B, 20 μl of biotin-labeled microtubule-like DNA structures (≈300 pM monomer concentration) and DNA origami drift markers (≈100 pM) in buffer B were finally flown into the chamber and incubated for 5 min. The chamber was washed using 40 μl of buffer B.

The final imaging buffer solution contained 1.5 nM Cy3b-labeled imager strands in buffer B. The chamber was sealed with epoxy before subsequent imaging. The CCD readout bandwidth was set to 1 MHz at 16 bit and 5.1 pre-amp gain. No EM gain was used. Imaging was performed using TIR illumination with an excitation intensity of 294 W/cm^2 at 561 nm.

Super-resolution Exchange-PAINT imaging of DNA nanostructures

For fluid exchange, a custom flow chamber was constructed as shown in Supplementary Figure 5. A detailed preparation protocol can be found in the Supplementary Protocol 1. Prior to functionalizing the imaging channel with BSA-biotin, it was rinsed with 1 M KOH for cleaning. Binding of the origami structures to the surface of the flow chamber was performed as described before. Each image acquisition step was followed with a brief ∼1–2 min washing step consisting of at least three washes using 200 μl of buffer B each. Then the next imager strand solution was introduced. The surface was monitored throughout the washing procedure to ensure complete exchange of imager solutions. Acquisition and washing steps were repeated until all ten targets were imaged. The CCD readout bandwidth was set to 3 MHz at 14 bit and 5.1 pre-amp gain. No EM gain was used. Imaging was performed using TIR illumination with an excitation intensity of 166 W/cm^2 at 561 nm (Ten-“color” Exchange-PAINT with 3 nM Cy3b-labeled imager strands in buffer B, Fig. 3c, d) and 600 W/cm^2 at 647 nm (Four-“color” Exchange-PAINT with 3 nM ATTO655-labeled imager strands in buffer B, Fig. 3e).

Super-resolution DNA-PAINT imaging of cells

All data was acquired with an EMCCD readout bandwidth of 5 MHz at 14 bit, 5.1 pre-amp gain and 255 electron-multiplying gain. Imaging was performed using HILO illumination[11]. The laser power densities were 283 W/cm^2 at 647 nm in Fig. 2a, 142 W/cm^2 at 647 nm and 19 W/cm^2 at 561 nm in Fig. 2d.

Imaging conditions: Fig. 2a: 700 pM ATTO655-labeled imager strands in buffer C. Fig. 2d: 600 pM Cy3b-labeled imager strands and 1.5 nM ATTO655-labeled imager strands in buffer C.

Super-resolution Exchange-PAINT imaging of cells

A Lab-Tek II chamber was adapted for fluid exchange as shown in Supplementary Figure 5. 2D images (Fig. 4a–d) were acquired with an EMCCD readout bandwidth of 5 MHz at 14 bit, 5.1 pre-amp gain and 255 EM gain. 3D images (Fig. 4f–h) were acquired with a CCD readout bandwith of 3 MHz at 154 bit, 5.1 pre-amp gain and no EM gain. Imaging was performed using HILO illumination in both cases. Sequential imaging was done as described for the 2D origami nanostructures, but the washing steps were performed using buffer C. The laser power densities at 647 nm were 257 W/cm^2 in Fig. 4a, 385 W/cm^2 in Figs. 4b, c, d. The laser power densities at 561 nm were 31 W/cm^2 in Figs. 4f, g, h.

Imaging conditions: Fig. 4a: 700 pM ATTO655-labeled imager strands in buffer C. Figs. 4b, c, d: 2 nM ATTO655-labeled imager strands in buffer C. Fig. 4f: 800 pM Cy3b-labeled imager strands in buffer C. Fig. 4g, h: 2 nM Cy3b-labeled imager strands in buffer C.

3D DNA-PAINT imaging

3D images were acquired with a cylindrical lens in the detection path (Nikon). The N-STORM analysis package for NIS Elements (Nikon) was used for data processing. Imaging was performed without additional magnification in the detection path, yielding 160 nm pixel size. 3D calibration was carried out according to the manufacturer's instructions.

Imager strand concentration determination

Optimal imager concentrations are determined empirically according to the labeling density. Generally, a high enough fluorescence OFF/ON-ratio has to be ensured in order to guarantee binding of only a single imager strand per diffraction-limited area. Additionally, a sufficient imager strand concentration (and thus sufficiently low fluorescence OFF-time) is necessary to ensure sufficient binding events and thereby robust detection of every docking strand during image acquisition.

Super-resolution data processing

Super-resolution DNA-PAINT images were reconstructed using spot-finding and 2D-Gaussian fitting algorithms programmed in LabVIEW[10]. A simplified version of this software is available for download at www.dna-paint.org.

Normalized cross-correlation analysis

Normalized cross-correlation coefficients were obtained by first normalizing the respective reconstructed gray-scale super-resolution images and subsequently performing a cross-correlation analysis in MATLAB R2013b (MathWorks, Natick, MA, USA).

Drift correction and channel alignment

DNA origami structures (Supplementary Figure 1) are used for drift correction and as alignment markers in in vitro DNA-PAINT and Exchange-PAINT imaging. Drift correction was performed by tracking the position of each origami drift marker throughout the duration of each movie. The trajectories of all detected drift markers were then averaged and used to globally correct the drift in the final super-resolution reconstruction. For channel alignment between different imaging cycles in Exchange-PAINT, these structures are used as alignment points by matching their positions in each Exchange-PAINT image.

For cellular imaging, 100 nm gold nanoparticles (Sigma Aldrich;10 nM in buffer C, added before imaging) were used as drift and alignment markers. The gold nanoparticles adsorb non-specifically to the glass bottom of the imaging chambers. Drift correction and alignment is performed in a similar fashion as for the origami drift markers. Again, the apparent movement of all gold nanoparticles in a field of view is tracked throughout the movie. The obtained trajectories are then averaged and used for global drift correction of the final super-resolution image. For the dual-color image of mitochondria and microtubules in Fig. 2d–f, the gold particles are visible in both color channels. The same gold nanoparticles are also used for drift-correction and re-alignment of the different imaging rounds in the *in situ* Exchange-PAINT experiments (Fig. 4).

Transmission electron microscopy imaging

For imaging, 3.5 µl of undiluted microtubules-like DNA structures were adsorbed for 2 minutes onto glow-discharged, carbon-coated TEM grids. The grids were then stained for 10 seconds using a 2 % aqueous ultra-filtrated (0.2 µm filter) uranyl formate solution containing 25 mM NaOH. Imaging was performed using a JEOL JEM-1400 operated at 80 kV.

Atomic force microscopy imaging

Imaging was performed using tapping mode on a Multimode VIII atomic force microscope (AFM) with an E-scanner (Bruker). Imaging was performed in TAE/Mg^{2+} buffer solution with DNP-S oxide-sharpened silicon nitride cantilevers and SNL sharp nitride levers (Bruker Probes) using resonance frequencies between 7–9 kHz of the narrow 100 µm, 0.38 N/m force constant cantilever. After self-assembly of the origami structure ≈20 µl of TAE/Mg^{2+} buffer solution was deposited onto a freshly cleaved mica surface (Ted Pella) glued to a metal puck (Ted Pella). After 30 s the mica surface was dried using a gentle stream of N_2 and 5 µl of the origami solution was deposited onto the mica surface. After another 30 s, 30 µl of additional buffer solution was added to the sample. Imaging parameters were optimized for best image quality while maintaining the highest possible setpoint to minimize damage to the samples. Images were post-processed by subtracting a 1st order polynomial from each scan line. Drive amplitudes were approximately 0.11 V, integral gains ≈2, and proportional gains ≈4.

Supplementary Material

Refer to Web version on PubMed Central for supplementary material.

Acknowledgments

We thank J. Nicoludis and M.T. Strauss for help with DNA origami design, T. Schlichthaerle for TEM imaging support, and M. Zhang for help with DLD1 cells. We also thank C. Steinhauer for help with DNA-PAINT software development and fruitful discussions. We thank R.D. Barish for critical reading and commenting on the manuscript. This work is supported by a National Institutes of Health (NIH) Director's New Innovator Award (1DP2OD007292), an NIH Transformative Research Award (1R01EB018659), an NIH grant (5R21HD072481), an Office of Naval Research (ONR) Young Investigator Program Award (N000141110914), ONR grants (N000141010827 and N000141310593), a National Science Foundation (NSF) Faculty Early Career Development Award (CCF1054898), an NSF grant (CCF1162459) and a Wyss Institute for Biologically Engineering Faculty Startup Fund to P.Y., and an NIH Director's New Innovator Award (1DP2OD004641) and a Wyss Institute for Biologically Inspired Engineering Faculty Award to W.M.S.. R.J. acknowledges support from the Alexander von Humboldt-Foundation through a Feodor-Lynen Fellowship. M.S.A. and M.D. acknowledge support from HHMI International Student Research Fellowships.

References

1. Rust MJ, Bates M, Zhuang X. Sub-diffraction-limit imaging by stochastic optical reconstruction microscopy (STORM). Nat Methods. 2006; 3:793–5. [PubMed: 16896339]
2. Hell SW. Microscopy and its focal switch. Nature methods. 2009; 6:24–32. [PubMed: 19116611]
3. Hell SW, Wichmann J. Breaking the diffraction resolution limit by stimulated emission: stimulated-emission-depletion fluorescence microscopy. Opt Lett. 1994; 19:780–2. [PubMed: 19844443]
4. Betzig E, et al. Imaging intracellular fluorescent proteins at nanometer resolution. Science. 2006; 313:1642–5. [PubMed: 16902090]
5. Sharonov A, Hochstrasser RM. Wide-field subdiffraction imaging by accumulated binding of diffusing probes. Proceedings of the National Academy of Sciences of the United States of America. 2006; 103:18911–18916. [PubMed: 17142314]
6. Giannone G, et al. Dynamic superresolution imaging of endogenous proteins on living cells at ultra-high density. Biophys J. 2010; 99:1303–10. [PubMed: 20713016]
7. Lew MD, et al. Three-dimensional superresolution colocalization of intracellular protein superstructures and the cell surface in live Caulobacter crescentus. Proc Natl Acad Sci U S A. 2011; 108:E1102–10. [PubMed: 22031697]
8. Flors C, Ravarani CN, Dryden DT. Super-resolution imaging of DNA labelled with intercalating dyes. Chemphyschem. 2009; 10:2201–4. [PubMed: 19554598]
9. Schoen I, Ries J, Klotzsch E, Ewers H, Vogel V. Binding-activated localization microscopy of DNA structures. Nano Lett. 2011; 11:4008–11. [PubMed: 21838238]
10. Jungmann R, et al. Single-Molecule Kinetics and Super-Resolution Microscopy by Fluorescence Imaging of Transient Binding on DNA Origami. Nano Letters. 2010; 10:4756–4761. [PubMed: 20957983]
11. Tokunaga M, Imamoto N, Sakata-Sogawa K. Highly inclined thin illumination enables clear single-molecule imaging in cells. Nature Methods. 2008; 5:159–161. [PubMed: 18176568]
12. Jungmann R, Scheible M, Simmel FC. Nanoscale imaging in DNA nanotechnology. Wiley Interdiscip Rev Nanomed Nanobiotechnol. 2012; 4:66–81. [PubMed: 22114058]
13. Lin C, et al. Submicrometre geometrically encoded fluorescent barcodes self-assembled from DNA. Nat Chem. 2012; 4:832–9. [PubMed: 23000997]
14. Derr ND, et al. Tug-of-war in motor protein ensembles revealed with a programmable DNA origami scaffold. Science. 2012; 338:662–5. [PubMed: 23065903]
15. Johnson-Buck A, et al. Super-resolution fingerprinting detects chemical reactions and idiosyncrasies of single DNA pegboards. Nano Lett. 2013; 13:728–33. [PubMed: 23356935]
16. Xu K, Babcock HP, Zhuang X. Dual-objective STORM reveals three-dimensional filament organization in the actin cytoskeleton. Nat Methods. 2012; 9:185–8. [PubMed: 22231642]
17. Vaughan JC, Jia S, Zhuang X. Ultrabright photoactivatable fluorophores created by reductive caging. Nat Methods. 2012; 9:1181–4. [PubMed: 23103881]
18. Rothemund PW. Folding DNA to create nanoscale shapes and patterns. Nature. 2006; 440:297–302. [PubMed: 16541064]

19. Douglas SM, et al. Self-assembly of DNA into nanoscale three-dimensional shapes. Nature. 2009; 459:414–418. [PubMed: 19458720]
20. Steinhauer C, Jungmann R, Sobey TL, Simmel FC, Tinnefeld P. DNA origami as a nanoscopic ruler for super-resolution microscopy. Angewandte Chemie (International ed in English). 2009; 48:8870–8873. [PubMed: 19830751]
21. Aitken CE, Marshall RA, Puglisi JD. An oxygen scavenging system for improvement of dye stability in single-molecule fluorescence experiments. Biophys J. 2008; 94:1826–35. [PubMed: 17921203]
22. Rasnik I, McKinney SA, Ha T. Nonblinking and long-lasting single-molecule fluorescence imaging. Nat Methods. 2006; 3:891–3. [PubMed: 17013382]
23. Vogelsang J, et al. A reducing and oxidizing system minimizes photobleaching and blinking of fluorescent dyes. Angew Chem Int Ed Engl. 2008; 47:5465–9. [PubMed: 18601270]
24. Ries J, Kaplan C, Platonova E, Eghlidi H, Ewers H. A simple, versatile method for GFP-based super-resolution microscopy via nanobodies. Nat Methods. 2012; 9:582–4. [PubMed: 22543348]
25. Wu N, et al. Molecular threading and tunable molecular recognition on DNA origami nanostructures. J Am Chem Soc. 2013; 135:12172–5. [PubMed: 23924191]
26. Kao HP, Verkman AS. Tracking of single fluorescent particles in three dimensions: use of cylindrical optics to encode particle position. Biophys J. 1994; 67:1291–300. [PubMed: 7811944]
27. Huang B, Wang W, Bates M, Zhuang X. Three-dimensional super-resolution imaging by stochastic optical reconstruction microscopy. Science. 2008; 319:810–3. [PubMed: 18174397]
28. Lubeck E, Cai L. Single-cell systems biology by super-resolution imaging and combinatorial labeling. Nat Methods. 2012; 9:743–8. [PubMed: 22660740]
29. Bates M, Dempsey GT, Chen KH, Zhuang X. Multicolor Super-Resolution Fluorescence Imaging via Multi-Parameter Fluorophore Detection. Chemphyschem : a European journal of chemical physics and physical chemistry. 2011; 13:99–107. [PubMed: 22213647]
30. Schweller RM, et al. Multiplexed in situ immunofluorescence using dynamic DNA complexes. Angew Chem Int Ed Engl. 2012; 51:9292–6. [PubMed: 22893271]
31. Ke R, et al. In situ sequencing for RNA analysis in preserved tissue and cells. Nat Methods. 2013; 10:857–60. [PubMed: 23852452]
32. Opazo F, et al. Aptamers as potential tools for super-resolution microscopy. Nat Methods. 2012; 9:938–9. [PubMed: 23018995]
33. Kazane SA, et al. Site-specific DNA-antibody conjugates for specific and sensitive immuno-PCR. Proc Natl Acad Sci U S A. 2012; 109:3731–6. [PubMed: 22345566]
34. Beliveau BJ, et al. Versatile design and synthesis platform for visualizing genomes with Oligopaint FISH probes. Proc Natl Acad Sci U S A. 2012; 109:21301–6. [PubMed: 23236188]

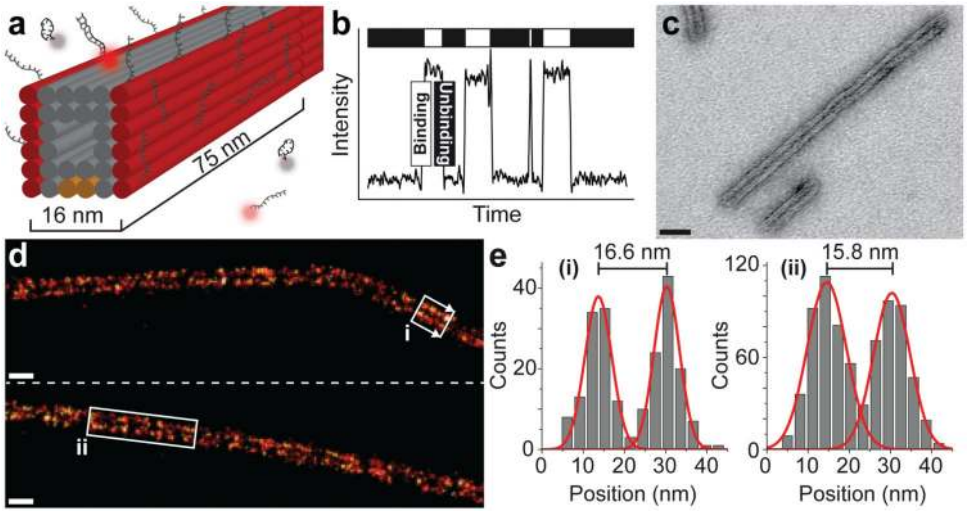

Figure 1.

DNA-PAINT. (**a**) A microtubule-like DNA origami polymer (cylinders represent DNA double helices) is decorated with single-stranded extensions (docking strands) on two opposite faces (colored in red) spaced ≈16 nm apart. Complementary fluorescent imager strands transiently bind from solution to docking strands. Biotinylated strands (present on orange colored helices) immobilize the structures to glass surfaces for fluorescence imaging. (**b**) Transient binding between imager and docking strands produces fluorescence blinking, allowing stochastic super-resolution imaging. (**c**) TEM image of origami polymers with a measured width of 16 ± 1 nm (mean ± stdv). Scale bar: 40 nm. (**d**) DNA-PAINT super-resolution images obtained using Cy3b-labeled imager strands (15,000 frames, 5 Hz frame rate). Two distinct lines are visible. Scale bars: 40 nm. (**e**) Cross-sectional histograms of highlighted areas <i> and <ii> in **d** (arrows denoting histogram direction) both reveal designed distance of ≈16 nm (FWHM of each distribution is ≈7–10 nm).

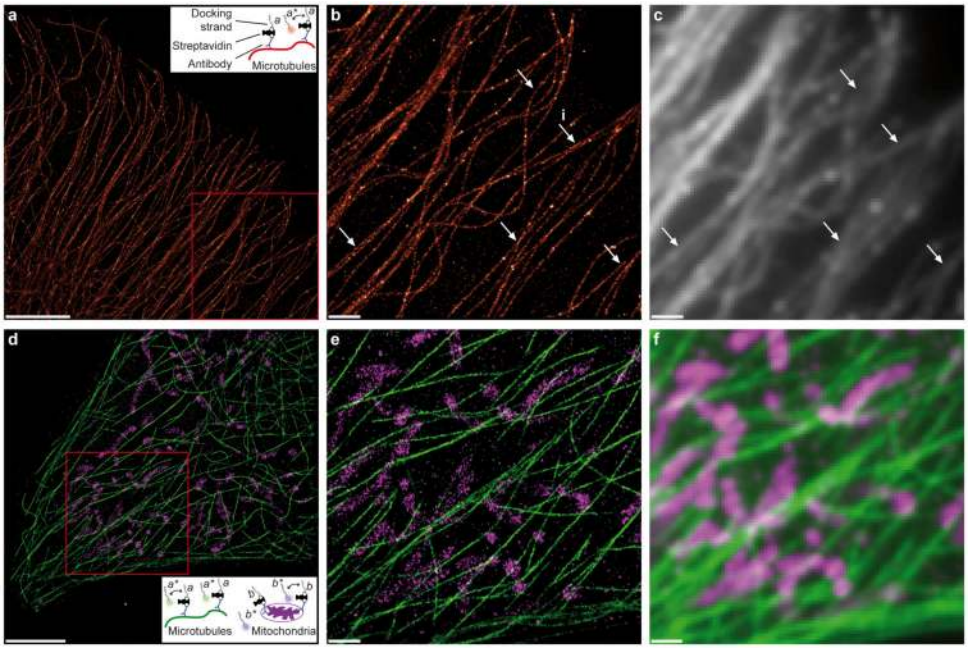

Figure 2.

Spectrally multiplexed DNA-PAINT super-resolution imaging of microtubules and mitochondria inside fixed cells. (**a**) DNA-PAINT super-resolution image of microtubules inside a fixed HeLa cell using Atto655-labeled imager strands (10,000 frames, 10 Hz frame rate). Scale bar: 5 μm. Inset: Labeling and imaging schematic for DNA-PAINT in a cellular environment. Microtubules are labeled with a pre-assembled antibody-DNA conjugate, which is formed between a biotinylated anti-tubulin antibody and a biotinylated DNA docking strand using a streptavidin bridge. (**b**) Zoom-in of the highlighted area in **a**. Scale bar: 1 μm. (**c**) Diffraction-limited representation of the same area as in **b**. Arrows highlight positions where the increase in resolution of the DNA-PAINT image is clearly visible. Adjacent microtubules with an apparent width of ≈46 nm at position <i> are separated by ≈79 nm (see Supplementary Figure 5 for enlarged image and quantification details). Scale bar: 1 μm. (**d**) Dual-color DNA-PAINT super-resolution image (15,000 frames, 10 Hz frame rate) of microtubules and mitochondria inside a fixed HeLa cell obtained using Cy3b-labeled imager strands for microtubules (green) and orthogonal ATTO655-labeled imager strands for mitochondria (magenta). Scale bar: 5 μm. Inset: Labeling and imaging schematic. (**e**) Zoom-in of the highlighted area in **d**. Scale bar: 1 μm. (**f**) Diffraction-limited image of the same area as in **e**. Scale bar: 1 μm.

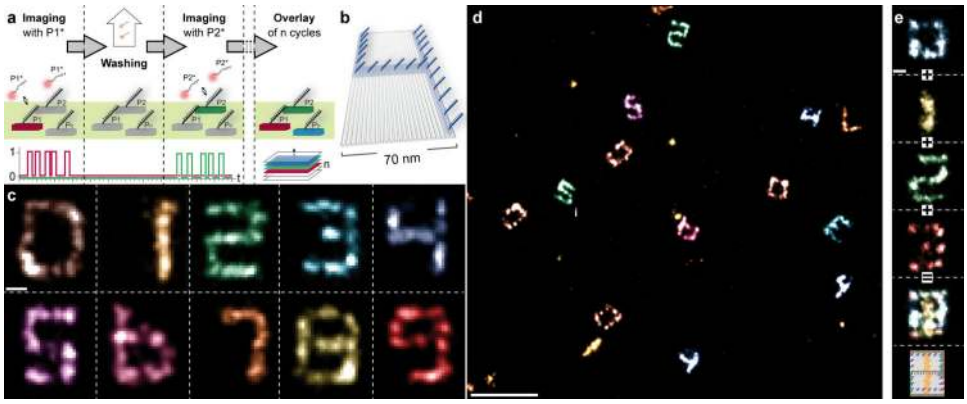

Figure 3.

Exchange-PAINT. (**a**) Exchange-PAINT schematic. Targets are labeled with orthogonal docking strands (P1, P2, etc.). In the first imaging round, only imager strands P1* are present and targets P1 are specifically imaged (Binarized intensity vs. time traces at the bottom show specific blinking of only P1 targets) and assigned a red pseudocolor. After acquisition, P1* strands are washed out and exchanged with imager strands P2*, and targets P2 are specifically imaged and assigned a green pseudocolor. All imager strands are labeled with the same fluorophore. Imaging and washing is repeated until all targets are imaged. A distinct pseudocolor is assigned in each imaging round. (**b**) Schematic of a DNA origami (70 × 100 nm) displaying docking strands that resemble digit 4. (**c**) Pseudocolor images of ten different origamis displaying digits 0 to 9 in one sample with high resolution (FWHM of bar-like features < 10 nm) and specificity. Image obtained using only one fluorophore (Cy3b) through ten imaging-washing cycles (imaging: 7,500 frames per cycle, 5 Hz frame rate; washing: 1-2 minutes per cycle). Scale bar: 25 nm. (**d**) Combined overview image of all ten Exchange-PAINT cycles, demonstrating specific interaction with the respective target with no crosstalk between imaging cycles. Scale bar: 250 nm. (**e**) Four-“color” image of digits 0 to 3 that are all present on the same DNA origami (10,000 frames each, 5 Hz frame rate; schematic at the bottom). Scale bar: 25 nm.

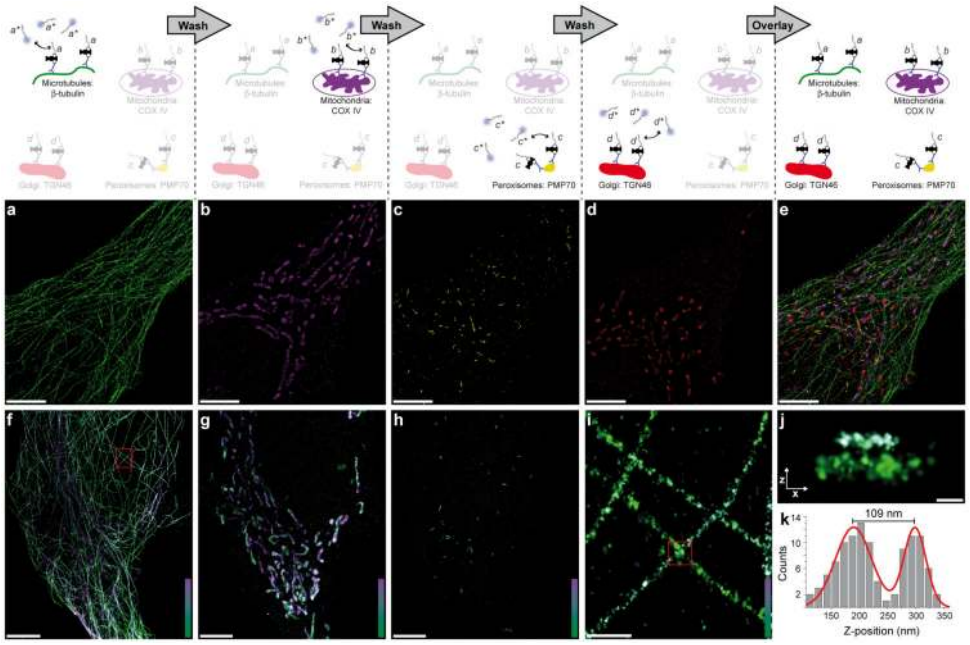

Figure 4.

Multiplexed 2D and 3D Exchange-PAINT super-resolution imaging in fixed cells. (**Top**) Schematic of experimental procedure. (**Center**) 2D Exchange-PAINT images. (**Bottom**) 3D Exchange-PAINT images. Each target is labeled with an antibody carrying a unique DNA-PAINT docking sequence. 2D and 3D imaging is performed using imager strands labeled with ATTO655 and Cy3b, respectively. (**a–e**) Four-"color" 2D images using ATTO655-labeled imager strands. (**a**) Only imager strands *a** are present, and microtubules are specifically imaged. (**b**) After washing out imager strands *a**, imager strands *b** are introduced and COX IV proteins in mitochondria are imaged. TGN46 proteins in the Golgi complex (**c**) and PMP70 proteins in peroxisomes (**d**) are imaged in the same way (Imaging: 15,000 frames per cycle, 10 Hz imaging rate; washing: 1-2 minutes per cycle). (**e**) Overlay of all four targets. (**f–k**) 3-"color" 3D images using Cy3b-labeled imager strands. (**f**) 3D image of microtubules, color indicates height. Height scale: 0 nm – 800 nm. (**g**) 3D image of mitochondria. Height scale: 40 nm – 1100 nm. (**h**) 3D image of peroxisomes. Height scale: 0 nm – 700 nm. (**i**) Zoom-in of the highlighted area in **f**. Height scale: 0 nm – 700 nm. (**j**) X-Z-profile of the highlighted area in **i**. (**k**) A two-component Gaussian fit reveals a distance of ≈109 nm in z of two adjacent microtubules. For 3D imaging: 50,000 frames per cycle, 16 Hz imaging rate; washing: 1-2 minutes per cycle. Scale bars in **a–h**: 5 μm; scale bar in **i**: 500 nm; scale bar in **j**: 100 nm.